

# Analysis of residual fabrication errors for computer controlled polishing aspherical mirrors

Xuejun Zhang

Jingchi Yu, MEMBER SPIE

Zhongyu Zhang

Quandou Wang

Weiping Zheng

Chang Chun Institute of Optics and Fine Mechanics

State Key Laboratory of Applied Optics

P.O. Box 1024

Chang Chun 130022, Jilin, China

E-mail: ccgjs@public.cc.jl.cn

**Abstract.** A quantitative expression for residual errors and mid-spatial-frequency errors of the aspherical surface finished by computer controlled polishing (CCP) is discussed in terms of the power spectral density model. The relationship between the magnitude of these errors and the CCP parameters is investigated using experimentation. An optimized CCP process is presented to reduce the residual surface errors. By properly choosing the polishing parameters such as tool size and lap material the residual errors can be removed. The final surface error of a hyperbolic mirror has reached 0.038 wave rms with residual errors less than 0.018 wave rms. © 1997 Society of Photo-Optical Instrumentation Engineers. [S0091-3286(97)03412-0]

Subject terms: computer controlled polishing; power spectral density; residual errors.

Paper 23047 received Apr. 22, 1997; revised manuscript received Aug. 5, 1997; accepted for publication Aug. 7, 1997.

## 1 Introduction

Computer controlled polishing (CCP) has been proven an efficient process to produce aspherical surfaces. In this process, the desired material removal is accurately achieved by allocating the proper tool dwell time on the workpiece surface with respect to the surface error height. Since the process is controlled by the computer, it is more accurate and time-saving than the conventional polishing process, which depends heavily on the optician's skills and experiences.

However, since a small tool rather than a large tool is used, the CCP process presents some problems which are not encountered in the conventional polishing process. The surface error structure, for example, is different from that of the surface finished by conventional polishing in which a large tool is employed. It is found that optical surface polished by CCP may contain higher "mid"-spatial-frequency errors than the surface polished in a conventional way. These errors span the gap between the "figure" and "finish" errors and degrade the achievable resolution of many imaging system.<sup>1</sup> These errors must be removed even though the conventional optics specifications such as rms and P-V have met the requirements.

A lot of attention has been paid to the optimizations of CCP parameters and machine configurations.<sup>2,3</sup> Also, the power spectral density (PSD) theory and its application in optical measurement have been extensively studied by others.<sup>4-6</sup> The purpose of this paper is to link the PSD model with the CCP process, to investigate and better understand the relationship between the magnitude of "mid"-frequency errors and the CCP parameters. Two major factors, tool size and tool material properties, which are closely related to the "mid"- and high-frequency errors, are discussed. Based on experiments, an optimized parameter collection is given to reduce the "mid"- and high-frequency errors. As an application, a hyperbolic mirror (fused silica) was polished with the modified CCP param-

eters. Both rms, "mid"- and high-frequency errors of the finished surface have met the requirements.

## 2 Representation of Wavefront

### 2.1 Zernike Polynomial Model

Most of the commercial interferometers employ optical phase shifting technique to calculate the phase.<sup>6</sup> The detector usually has a dimension of 512×512 or 256×256 pixels. The intensity at each pixel of the detector has the following form:

$$I(x,y) = a + b \cos[\varphi(x,y) + \alpha]$$

where  $a$  is a constant,  $b$  is the fringe contrast,  $\varphi(x,y)$  is the phase at the point  $(x,y)$ , and  $\alpha$  is the initial phase. Generally, the "four-step algorithm" for phase calculation is briefly expressed as:

$$I_1(x,y) = a + b \cos[\varphi(x,y) + 0]$$

$$I_2(x,y) = a + b \cos\left[\varphi(x,y) + \frac{\pi}{2}\right]$$

$$I_3(x,y) = a + b \cos[\varphi(x,y) + \pi]$$

$$I_4(x,y) = a + b \cos\left[\varphi(x,y) + \frac{3\pi}{2}\right]$$

then the phase at each pixel is given by:

$$\varphi(x,y) = \arctan\left(\frac{I_4 - I_2}{I_1 - I_3}\right). \quad (1)$$

The phase can be converted into the height variations by:

$$W_{\text{measured}}(x,y) = \frac{\lambda}{4\pi} \varphi(x,y). \quad (2)$$

Keep in mind that the height values given by Eq. (2) are discrete over the optical surface. To aid in the interpretation of the test results, wavefront shape has been expressed by fitting those discrete values in terms of Zernike polynomials:

$$W_{\text{fitted}}(x,y) = \sum_{n=1}^k a_n U_n(x,y) \quad (3)$$

where  $W_{\text{fitted}}(x,y)$  is surface error distribution function,  $a_n$  is Zernike coefficients,  $U_n(x,y)$  is Zernike polynomials, and  $k$  is the number of terms, usually  $k=36$ . It is agreeable that Zernike polynomials correctly express the low-spatial-frequency errors commonly recognized as ‘‘shape’’ or ‘‘figure,’’ of which the spatial wavelengths range from  $D$  down to approximately  $D/12$ , where  $D$  is the diameter of the workpiece. However, the mid-spatial-frequency errors (‘‘ripple,’’ spatial wavelengths range from  $D/12$  to  $D/40$ ) and the high-spatial-frequency errors (spatial wavelengths are shorter than  $D/40$ ) are expressed only as ‘‘residuals’’ of the polynomial fit.<sup>6</sup> The rms value of these residual errors can be expressed as:

$$\text{rms}_{\text{residual}} = \sqrt{\frac{1}{N \times M} \sum_{n=1}^N \sum_{m=1}^M (W_d(x_n, y_m) - S)^2}$$

$$W_d(x_n, y_m) = W_{\text{measured}}(x_n, y_m) - W_{\text{fitted}}(x_n, y_m) \quad (4)$$

$$S = \frac{1}{N \times M} \sum_{n=1}^N \sum_{m=1}^M W_d(x_n, y_m).$$

Note that the information about the mid-spatial-frequency and the high-spatial-frequency errors is lost after Zernike fitting. In this case Zernike polynomials become less effective and the power spectral density (PSD) is introduced to analyze the error components with specified frequencies.

## 2.2 PSD Model to Analyze the Surface Error Structure

The power spectral density (PSD) is a powerful and compact expression of wavefront structure,<sup>6</sup> expressing the contour of the wavefront ‘‘phase surface’’ in terms of Fourier component. With this tool one can easily analyze the surface errors within any frequency range if the data is valid. In this paper the discussion will focus on calculating one-dimensional PSD from the profile data provided by a Zygo interferometer (readers are referred to Ref. 4 for the extension from one-dimensional PSD to two-dimensional PSD).

In one-dimension, the magnitude of the PSD at a specified frequency  $k_i$  is given by:

$$\text{PSD}(k_i) = \frac{[Z(k_i)]^2}{\Delta k} \quad (5)$$

where  $Z(k_i)$  is the discrete Fourier amplitude at the frequency  $k_i$ , which can be expressed by the Fourier transform:

$$Z(k) = \int_0^L W(x) e^{-ikx} dx. \quad (6)$$

Let  $N$  equal the number of sampling points, and  $\Delta x$  represent equally spaced intervals over the total length  $L$ , then  $L = N\Delta x$ .  $\Delta k$  is the increment between frequencies and is equal to  $1/L$ . As mentioned above, what we are interested in is the mid-spatial-frequency errors that have a range of wavelengths from  $D/12$  down to  $D/40$ . According to Elson and Aikens,<sup>4,5</sup> it can be shown that the ‘‘area’’ under the PSD curve in any frequency interval is equal to the square of the rms wavefront error of the original line-out over the same frequency interval, so we have:

$$\text{rms}^2 = (\Delta k) \times \sum_{i=1}^N \text{PSD}(k_i). \quad (7)$$

With Eqs. (5) to (7) we are able to calculate the magnitude of the mid-spatial-frequency errors.

So far we have discussed the method of analyzing the surface error structure. In the following section we will discuss the relationship between the magnitude of the mid-spatial-frequency errors and the CCP parameters and also the optimization of the CCP process to remove these errors.

## 3 Optimization of CCP Process to Correct Mid-Spatial-Frequency Errors

### 3.1 Characterization of the Optical Surface Polished in a Traditional Way

Figure 1(a) shows the surface error map of a spherical surface corrected by conventional large tool polishing. Figure 1(b) is the result fitted by 36 Zernike polynomials. The residual rms error calculated by Eq. (4) is 0.015 wave, where wavelength is  $0.6328 \mu\text{m}$ . Based on Eq. (4), the standard FFT technique was used to calculate the magnitude of the mid-frequency errors. Generally, the sampling length  $L_0$  is less than 256 when the test is performed on a Zygo interferometer. To increase the resolution in the frequency domain the actual analyzing length was extended to 256 by ‘‘padding’’  $M$  zeros, where  $M = 256 - L_0$ . Therefore the frequency resolution will be:

$$\Delta k = \frac{L_0}{D \times 256}$$

where  $D$  is the workpiece diameter.

Figure 1(c) is the graph of normalized PSD versus spatial frequency. The rms value of the mid-frequency errors is 0.01 wave. This surface has proven to be acceptable in the imaging system.

### 3.2 Aspherical Surface Corrected by CCP Process

The polishing tool diameter used in the CCP process usually ranges from  $D/15$  to  $D/8$ , where  $D$  is the workpiece’s

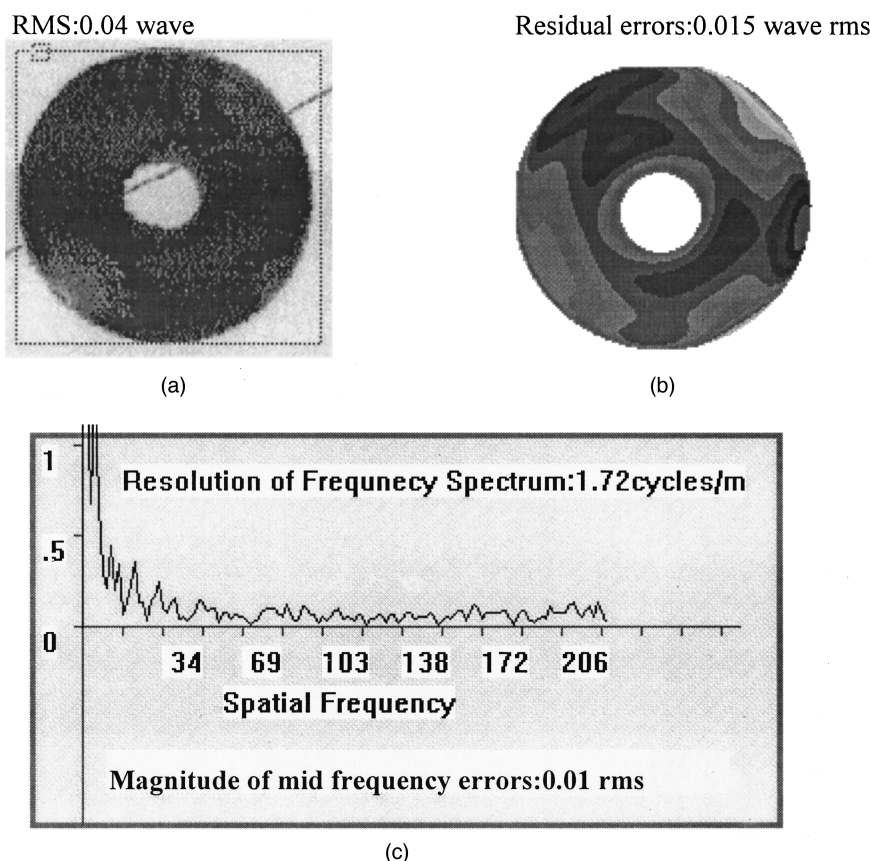


**Fig. 1** Characterization of a spherical surface polished in a conventional way. (a) Surface error map of a spherical surface. (b) Zernike fitting result. (c) Graph of normalized PSD versus spatial frequency.

diameter. In addition, relatively soft lap material is used to allow adequate pitch flow. These two conditions will make the tool effectively follow the workpiece shape and correct the low-spatial-frequency errors efficiently. The schematic drawing of this process is shown in Fig. 2. Figure 3(a) is the original errors of a hyperbolic mirror with a diameter of 200 mm and f number of 1/4. After 30 polishing hours the errors has been corrected to 0.05 wave rms, as shown in Fig. 3(b). When considering the conventional optics specifications such as rms and P-V, this surface has met the requirement. However, one can see it has higher residual errors than that of the surface polished in the traditional way. Figure 3(c) shows the Zernike fitted phase map. The residual errors are 0.045 wave rms. Furthermore, as shown

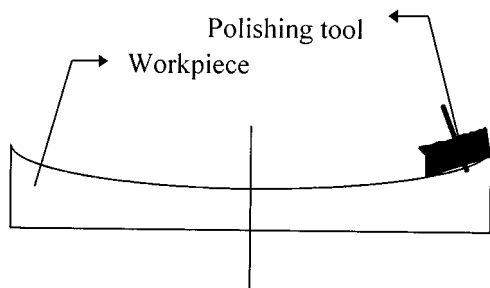


**Fig. 2** Schematic drawing of CCP process.

in Fig. 3(d), when analyzing the surface structure by means of PSD, the magnitude of mid-frequency errors is found higher than that of the spherical surface polished with a large tool. These residual errors, as mentioned above, will affect the imaging quality and must be removed. This goal could be achieved by properly choosing the CCP parameters.

### 3.3 Relationship Between Residual (Mid-Frequency) Errors and CCP Parameters

Unlike the conventional polishing, not only the traditional optics specifications such as rms and P-V, but also the surface residual errors and mid-frequency errors should be taken into account during the CCP process. Equations (4) to (7) have provided a quantitative means to analyze these errors. Our purpose is to find out the relation between the residual errors and the CCP parameters, and optimize the CCP process to remove these errors.

In the CCP experiment the mid-frequency errors have been found sensitive to two parameters: the tool size and the lap modulus. The total diameter in our experiment ranged from  $D/12$  to  $D/4$ . The experiment was performed on a FSGJ-1 CNC machine and a Zygo mark IV xp interferometer plus null compensator was used to test the surface errors. Figure 4 shows the experiment setup. Based on the discussion in Section 2 and the profile data offered by

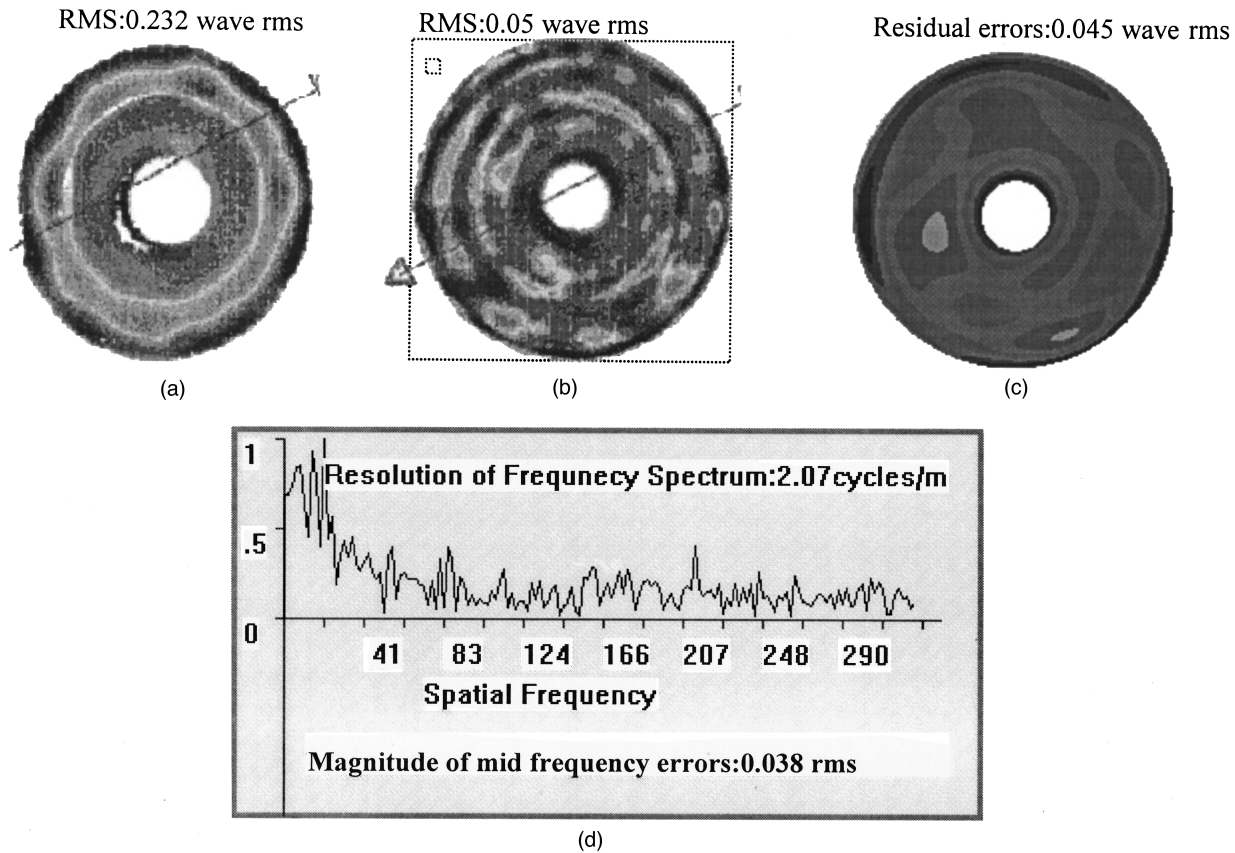
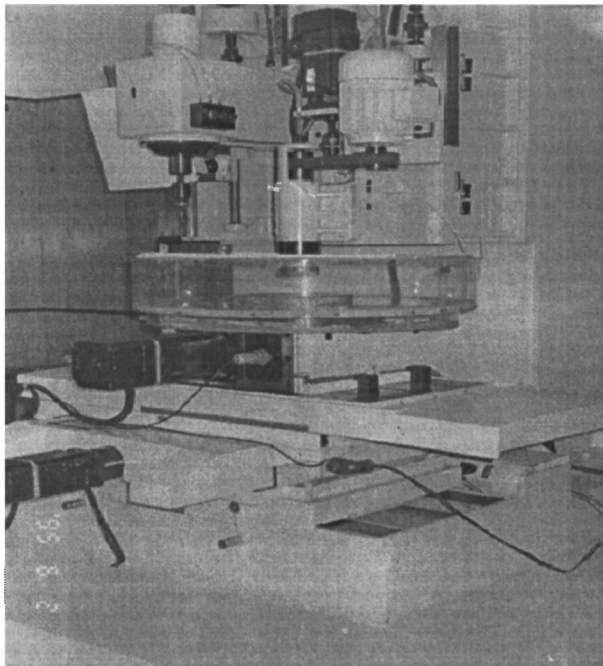


**Fig. 3** Characterization of hyperbolic surface by small tool CCP correction. (a) Original error map. (b) Error map after 30 CCP hours. (c) Zernike fitting result. (d) PSD plot versus spatial frequency.



**Experiment Setup**

**Fig. 4** Experimental setup.

Zygo, a computer program was written to calculate the residual errors and PSD of the workpiece surface.

First, the smaller tool with diameter ranging from  $D/12$  to  $D/8$  and lap modulus of 130 bar was used to polish the workpiece. As shown in Figs. 3(a) and 3(b) the surface error has been quickly reduced from 0.203 wave rms to 0.05 wave rms. Continuing to polish the workpiece without changing the parameters would not significantly improve the surface figure, however, as shown in Figs. 3(c) and 3(d), the residual errors and the mid-frequency errors were higher than that of the surface polished in the conventional way. Figure 5 shows the graph of residual errors and magnitude of mid-frequency errors versus the tool diameter and lap modulus. It is found that the residual errors or mid-frequency errors decrease as the tool diameter increases, but the curve levels off when the tool diameter becomes larger than  $D/4$ . As shown in Fig. 5(b), the effect of lap modulus on the residual errors and mid-frequency errors is similar to that of the tool size but is less intensive. This indicates that larger tool and harder lap have a good effect on smoothing.<sup>7</sup> Figure 6 shows the final result of the hyperbolic surface finished by varying the tool diameter from  $D/8$  to  $D/4$  and the lap modulus from 130 bar to 240 bar. Compared to the data shown in Figs. 3(c) and 3(d), both residual errors and mid-frequency errors have been reduced to the same level of the surface polished in the conventional way.



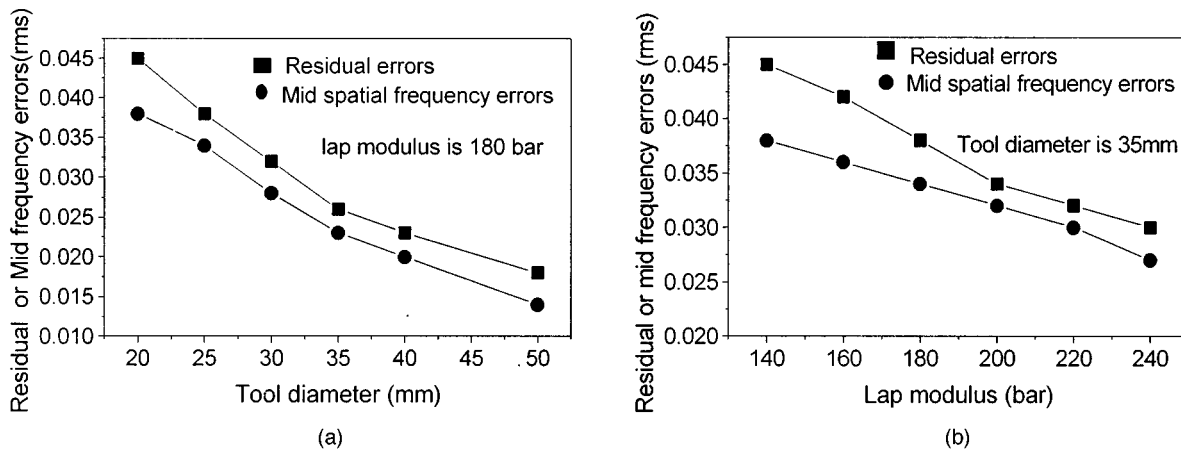


**Fig. 5** Relation between residual errors and CCP parameters. (a) Tool size role in removing residual errors. (b) Lap modulus role in removing residual errors.

The above discussion suggests that the CCP process with a small tool ( $D/10$ ) can be modified to remove the residual errors and mid-frequency errors. Generally, when the surface errors are worse than 0.05 wave rms, a smaller and softer lap is effective to correct low-frequency errors. In this case the traditional optics specifications such as rms and P-V will be used to evaluate

the polishing efficiency. When the surface errors are better than 0.05 wave rms, however, the mid-spatial-frequency errors and residual errors become the major factor affecting the CCP efficiency, and a larger and harder lap should be used to improve the surface quality. A diagram of the optimized CCP process to remove the residual errors is shown in Fig. 7.

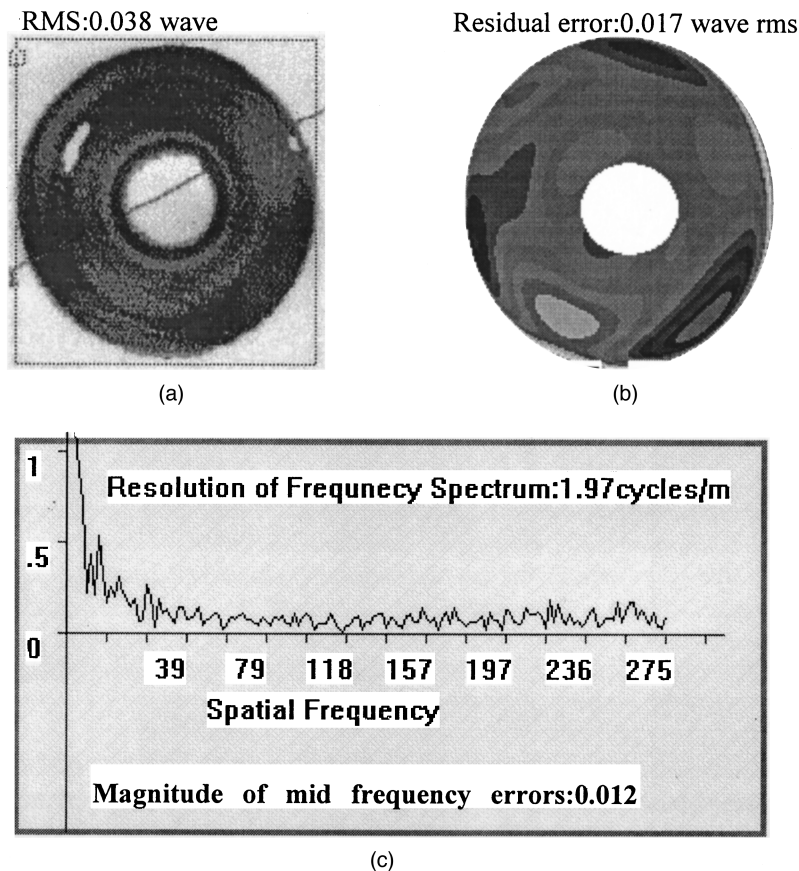


**Fig. 6** Characterization of the hyperbolic surface finished by modified CCP process. (a) Final error map. (b) Zernike fitting result. (c) PSD plot versus spatial frequency.

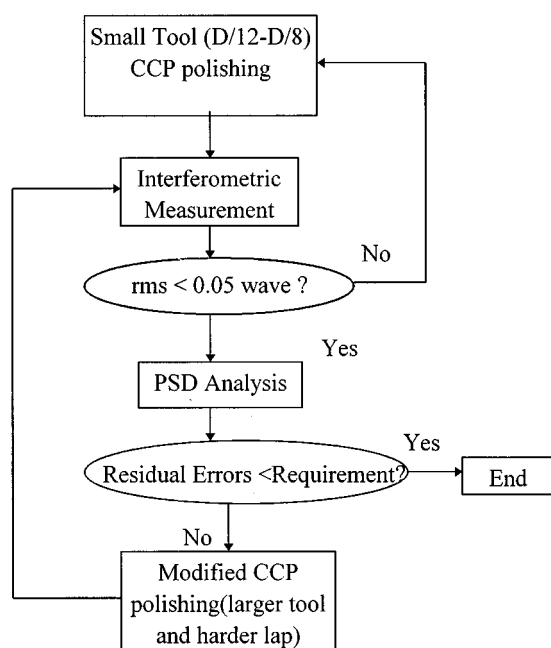


Fig. 7 Diagram of the optimized CCP process.

#### 4 Conclusions

The CCP process using a small tool produces higher residual errors and mid-frequency errors than traditional polishing processes, and these errors can be quantitatively expressed in terms of a PSD model. Based on this model the relation between the magnitude of the residual errors and the CCP parameters is determined by means of CCP polishing experiments. This relation provides a guide for properly choosing CCP parameters to improve surface quality. The final surface errors of the hyperbolic mirror finished by the optimized CCP process have reached 0.038 wave rms, and both residual errors and mid-frequency errors have been reduced to a level equivalent to a surface polished in a traditional way.

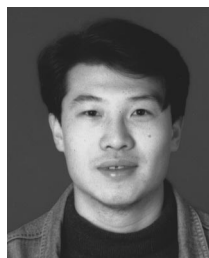
#### Acknowledgment

The authors would like to thank Prof. Weng Zhicheng and Prof. Sun Xiafei for their constructive suggestions and helpful discussions and Mrs. Wang Shurong for her help with experiments.

#### References

1. J. E. Harvey and A. Kotha, "Scattering effects from residual optical fabrication errors," *Proc. SPIE* **2576**, 155–174 (1995).
2. R. A. Jones, "Optimization of computer controlled polishing," *Appl. Opt.* **16**, 218–224 (1977).
3. R. Aspden, R. McDonough, and F. R. Nitchie, Jr., "Computer assisted optical surfacing," *Appl. Opt.* **11**, 2739–2747 (1972).

4. J. M. Elson and J. M. Bennett, "Calculation of power spectral density from surface profile data," *Appl. Opt.* **34**, 201–208 (1995).
5. D. M. Aikens, "The origin and evolution of the optics specifications for the National Ignition Facility," *Proc. SPIE* **2536**, 2–12 (1995).
6. J. K. Lawson, C. R. Wolfe, K. R. Manes, J. B. Trenholme, D. M. Aikens, and R. E. English, Jr., "Specification of optical components using the power spectral density function," *Proc. SPIE* **2536**, 38–50 (1995).
7. R. A. Jones, "Computer simulation of smoothing during computer-controlled optical polishing," *Appl. Opt.* **34**, 1162–1169 (1995).



**Xuejun Zhang** received his MS in engineering and is now a PhD candidate and working at the State Key Laboratory of Applied Optics, Chang Chun Institute of Optics and Fine Mechanics. His research interests include ultra-precision manufacturing, aspherical surface fabrication and testing, new optical materials and fabrication techniques, as well as computer applications. He has published more than 20 technical papers.



**Jingchi Yu** is a Professor at the State Key Laboratory of Applied Optics, Chang Chun Institute of Optics and Fine Mechanics. He is now in charge of a project on automated fabrication and testing of aspherics and has accomplished more than ten projects specialized in optical manufacturing and metrology.



**Zhongyu Zhang** is a mechanical engineer at the State Key Laboratory of Applied Optics. He has participated in more than five research projects regarding the design and fabrication of automated optical fabrication machines.



**Quandou Wang** is a graduate student specializing in optical metrology and testing. He is now engaged in a project on automated fabrication and testing of aspherics.

**Weiping Zheng** is a research assistant at Chang Chun Institute of Optics and Fine Mechanics. As a main investigator he has joined in many research projects regarding automated optical fabrication.